Articles

Vibrational Analysis of Dopamine Neutral Base based on Density Functional Force Field

Sun-Kyung Park, Nam-Soo Lee,* and Sang-Ho Lee†

Department of Chemistry, Chungbuk National University, Cheongju, Chungbuk 361-763, Korea
†Biophysics Research Division and Department of Physics, The University of Michigan, Ann Arbor, MI 48109, USA
Received July 27, 2000

Vibrational properties of dopamine neutral species in powder state have been studied by means of the normal mode analysis based on the force constants obtained from the density functional calculation at B3LYP level and the results of Fourier transform Raman and infrared spectroscopic measurements. *Ab initio* calculation at MP2 level shows that the *trans* conformer of dopamine has higher electronic energy about 1.4 kcal/mol than those of the *gauche*+ and the *gauche*− conformers, and two *gauche* conformers have almost the same energies. Free energies calculated at HF and B3LYP levels show very similar values for three conformers within 0.3 kcal/mol. Empirical force field has been constructed from force constants of three conformers, and refined upon experimental Raman spectrum of dopamine to rigorous values. The major species of dopamine neutral base in the powder state is considered a *trans* conformer as shown in the crystallographic study of dopamine cationic salt.

Introduction

Dopamine[1] serves as a neurotransmitter in the central and sympathetic nerve system or as a hormone in vesicles of the adrenal medulla for the regulation of the heart beat rate and blood pressure. It is a rather simple species of an ethylamine base connected to the catechol ring. It could contain a proton at the ethylamine moiety to be a cationic species, or lose one or two protons at two hydroxyl groups of the catechol ring moiety to be a monoanionic, dianionic, or zwitterion-like species. Dopamine could have three staggered conformations through an ethylamine side chain, *i.e.*, a stretched *trans*, and two folded *gauche* conformations for each species possible. The structure or conformations of dopamine and the functions of dopamine moieties for the biological activities have been in great interest in chemistry or biological neurosciences. The structural studies *via* the spectroscopic methods, for example, X-ray crystallography, nuclear magnetic resonance,[2] and Raman scattering,[2(c),3-5] or *via* the computational methods[6-12] have been carried out and reported. Much attention so far had almost been concentrated on the study of the ionic species of dopamine. Vibrational studies are relatively rare compared to the other methods, however. Raman spectroscopic studies of dopamine were also reported for the species adsorbed on the metal surfaces.[3-5] The vibrational analysis of any of the dopamine species has not been considerably studied yet so far.

Application[13-16] of density functional theory (DFT) to chemistry has received much attention recently because of a faster convergence in time than the traditional quantum mechanical correlation methods in part, and improvements in the prediction of the molecular force field, vibrational frequencies, and dipole moments. Therefore the force field from DFT calculation could be utilized with the spectroscopic data for the assignment of observed frequencies and the refinements of the molecular force field under study. The normal mode analysis[17,18] has been applied to elucidate the molecular system of chemistry and biological sciences using Wilson's *GF* matrix formulation.[19] This matrix method has been enforced with improvements in the setup of internal coordinates, or in the computational method in the refinement procedure of the force field. It is now in progress to expand its application area to molecular dynamics studies as well as structural studies.

In the present study, the vibrational analysis of dopamine neutral base was investigated by normal mode analysis method using the spectroscopic Raman data and the force field obtained from DFT calculation to clarify the vibrational structure and conformation in a powder state of neutral base form.

Experimental and Calculation Methods

Dopamine·HCl and NaOH were purchased of the highest purity from Tokyo Kasei Chemical and used as received without further purifications. To prepare sodium salt, dopamine·HCl was mixed with equivalent amount of NaOH solution, and dried in vacuum with cooling. Bruker FRA106 Fourier transform spectrometer was applied in dry nitrogen purge mode to obtain Raman spectrum. It was equipped with 1064 nm cw Nd : YAG laser, a calcium fluoride beam splitter and liquid nitrogen cooled InGaAs detector for Raman scattering. The laser power was about 0.2 watt at sample. The spectral resolution was set to 4 cm^{-1} and 100 times accumulated for each run. A sample powder was contained with tight packing for irradiation in ordinary melting point capillary tube (Drummond Scientific Co.). The infrared spectrum was obtained using the Bruker IFS66 machine with MCT

detector, Nernst bar light source and KBr beam splitter in the spectral resolution of 4 cm^{-1} and 100 times accumulated for each run.

Initial molecular structure was generated and optimized at AM1 level using the PC Spartan Plus (Wavefunction, Inc.) and transferred to the Gaussian package (Gaussian, Inc.) for the optimization at the higher levels. For the drawing, CS CHEM3D PRO (CambridgeSoft Cooperation) was utilized. The energy corresponding to an optimized geometry was obtained at HF, MP2, and B3LYP levels and using the 6-31G** basis set. Raw Cartesian force constants and the intensities of Raman and IR bands were obtained from a geometry optimized fully using B3LYP functional and 6-31G** basis set. Calculated Cartesian force constants were transformed to a set of force constants in non-redundant local symmetry coordinates for a refinement procedure. The refinement procedure[18] of raw force constants obtained from DFT calculation was carried out by minimizing the quantity χ^2,

$$\chi^2 \equiv \sum_{i=1}^{NOFQ} \{w(i) \cdot (\nu_i^{observed} - \nu_i^{calculated})\}^2$$

where *NOFQ* is the total number of observed frequencies ($\nu_i^{observed}$) to be considered and $w(i)$ is the weight factor for the frequency of the ith mode. The actual minimization of the quantity χ^2 was done by the conjugate gradient method with a cube interpolation in each line minimization using a least-square fitting program. Normal modes and frequencies of vibrations were calculated using the Wilson's *GF* matrix method.

Ab initio Calculation and Normal Mode Calculation

The chemical structure of dopamine in the neutral base form is shown in Figure 1 with an index number for each atom. It has been known that three staggered conformations shown in Figure 2, *i.e.*, *trans*, *gauche*- and *gauche*+ conformer are staged in each local minimum in energy. It can be described by two dihedral angles of the ethylamine moiety. Each conformer was optimized and the energies were calculated using HF, MP2 and B3LYP functions. Their relative energies to the minimum energy noted in 0.000 kcal/mol are displayed with dipole moments calculated by each function in Table 1.

Each conformation optimized at B3LYP/6-31G** level was applied to calculate the frequencies of the normal coordinates and the force constant matrix in Cartesian coordinate at the B3LYP level with the same basis set The isotope atomic masses adapted were 12.01115 for carbon, 14.00307 for nitrogen, 15.9994 for oxygen, and 1.007825 for hydrogen, respectively. The temperature was set to 298.15 K and the pressure to 1.0 atm. Raman spectra of three conformers obtained initially by calculation are shown in Figure 3. Each band displayed in Figure 3 was shaped according to the Lorentz line shape ($R(\omega) = (FWHH/2)^2/\{(\omega_o - \omega)^2 + (FWHH/2)^2\}$, FWHH: the full width at half-height, ω_o = a resonant frequency) with the full-width at half height, 5.0 cm^{-1}. With applying the scale factor of 0.96 to the frequencies obtained from DFT calculation, the Raman spectra of three staggered

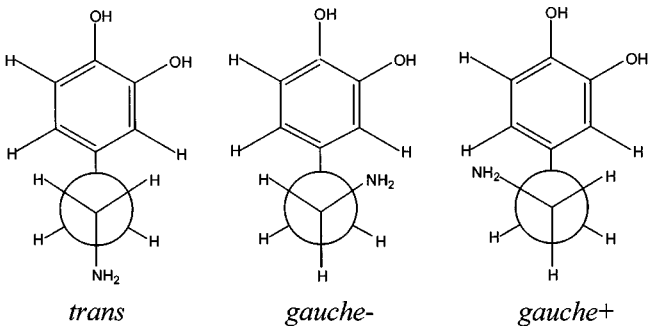

Figure 2. Three staggered conformations (*trans*, *gauche*-, and *gauche*+) of dopamine neutral base.

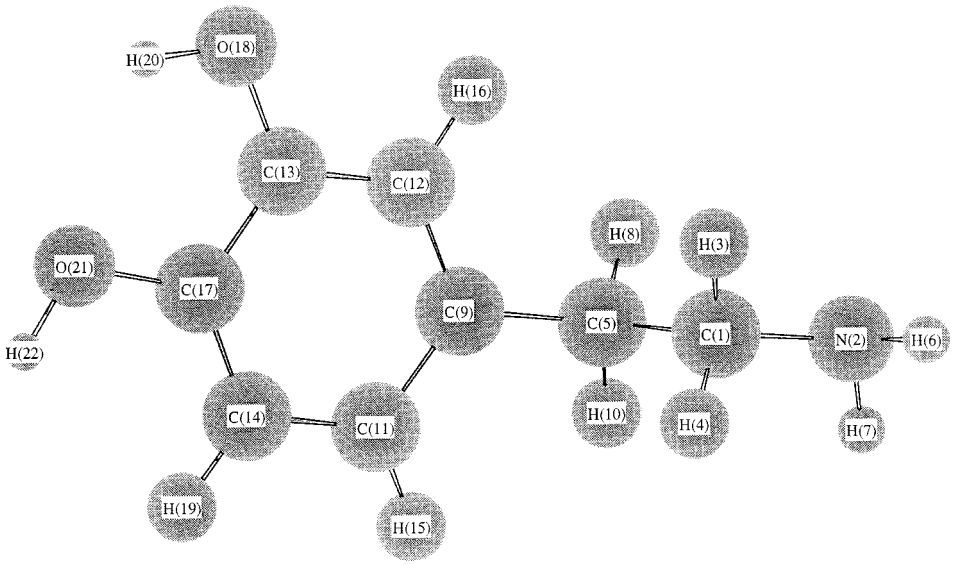

Figure 1. Molecular structure of dopamine neutral base in the *trans* conformation with index numbers.

Table 1. Calculated Relative Energies and Dipole moments at 298.15 K and 1.0 atm for Three Conformers of Dopamine neutral base, *trans*, *gauche*+ and *gauche*–

Dopamine Neutral Base		trans	*gauche*$^+$	*gauche*$^-$
HF/6-31G**	ΔE_{elec}/kcal/mol*	0.116	**0.000**	0.021
	ZPC/Hartree	0.196171	0.196386	0.196358
	ΔE_T/kcal/mol	0.094	**0.000**	0.016
	ΔH_T/kcal/mol	0.094	**0.000**	0.016
	ΔG_T/kcal/mol	**0.000**	0.239	0.215
	Dipole/Debye	3.6259	3.4291	2.8607
MP2/6-31G**	ΔE_{elec}/kcal/mol	1.366	0.018	0.000
	Dipole/Debye	3.8801	3.4759	3.0718
B3LYP/6-31G**	ΔE_{elec}/kcal/mol	0.938	0.021	**0.000**
	ZPC/Hartree	0.182956	0.183285	0.183280
	ΔE_T/kcal/mol	0.885	0.032	**0.000**
	ΔH_T/kcal/mol	0.885	0.032	**0.000**
	ΔG_T/kcal/mol	0.326	**0.000**	0.013
	Dipole/Debye	3.4011	3.2184	2.8876

*ΔE_{elec}: relative electronic energy, ZPC: zero-point correction energy, ΔE_T: relative summation of electronic and thermal energies, ΔH_T: relative summation of electronic and thermal enthalpies, ΔG_T: relative summation of electronic and thermal free energies.

conformations are displayed in Figure 3. The Raman intensities obtained initially from the DFT calculation were scaled for the better view to the tenth power of the inverse of frequency difference from the laser excitation line 1064 nm because the Raman band intensities located in the stretching region above 2800 cm^{-1} were calculated with huge amounts.

The internal coordinates of dopamine of total 22 atoms consist of 22 stretching coordinates (Δr) numbered R1 to R22, 35 in-plane deformation coordinates ($\Delta\theta$) numbered R23 to R57, 9 out-of-plane deformation coordinates ($\Delta\omega$) numbered R58 to R66, and 11 torsion coordinates ($\Delta\tau$) numbered R67 to R77. They are defined based on the atomic numbering scheme in Figure 1 and shown in Table 2 with molecular structural parameters of the *trans* conformer for reference.

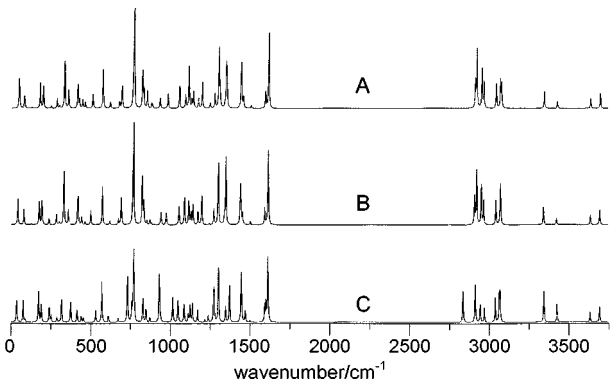

Figure 3. Raman spectra of three staggered conformations scaled with a scale factor 0.96 for vibrational frequencies obtained initially from the DFT calculations; (A) *gauche*-, (B) *gauche*+, and (C) *trans*. Each peak was adjusted to the Lorentz line shape with FWHH 5.0 cm^{-1}, and the intensities obtained from the DFT calculations were scaled to the frequency difference from 1064 nm excitation laser wavelength.

The local symmetry coordinates adapted for dopamine are shown in the format of non-normalized in Table 3 with descriptions in terms of the internal coordinates R defined in Table 2. Here, we did not utilize the symmetry property of the benzene ring because the catechol moiety of dopamine is a tri-substituted ring system. Each localized chemical bond in the catechol ring was regarded as a local symmetry coordinate, instead. A complete set of 60 local symmetry coordi-

Table 2. Internal Coordinates of Dopamine (R: the index number of internal coordinates, Atoms: the index number indicated in Figure 1.) and Molecular Structural Parameters

R	Name[a]	Atoms		R	Name	Atoms	
1	Δr(C-N)	1-2	(1.466 Å)[b]	40	$\Delta\theta$(CCC)	11-9-12	(118.6°)
2	Δr(C-C)	1-5	(1.538 Å)	41	$\Delta\theta$(CCC)	9-11-14	(120.9°)
3	Δr(C-H)	1-3	(1.096 Å)	42	$\Delta\theta$(CCH)	9-11-15	(119.8°)
4	Δr(C-H)	1-4	(1.105 Å)	43	$\Delta\theta$(CCH)	14-11-15	(119.3°)
5	Δr(N-H)	2-6	(1.017 Å)	44	$\Delta\theta$(CCC)	9-12-13	(121.0°)
6	Δr(N-H)	2-7	(1.018 Å)	45	$\Delta\theta$(CCH)	9-12-16	(120.8°)
7	Δr(C-C)	5-9	(1.513 Å)	46	$\Delta\theta$(CCH)	13-12-16	(118.1°)
8	Δr(C-H)	5-8	(1.095 Å)	47	$\Delta\theta$(CCC)	12-13-17	(119.5°)
9	Δr(C-H)	5-10	(1.098 Å)	48	$\Delta\theta$(CCO)	12-13-18	(120.1°)
10	Δr(C~C)	9-11	(1.398 Å)	49	$\Delta\theta$(CCO)	17-13-18	(120.3°)
11	Δr(C~C)	9-12	(1.403 Å)	50	$\Delta\theta$(CCC)	11-14-17	(119.9°)
12	Δr(C~C)	11-14	(1.399 Å)	51	$\Delta\theta$(CCH)	11-14-19	(120.4°)
13	Δr(C-H)	11-15	(1.086 Å)	52	$\Delta\theta$(CCH)	17-14-19	(119.8°)
14	Δr(C~C)	12-13	(1.391 Å)	53	$\Delta\theta$(CCC)	13-17-14	(120.1°)
15	Δr(C-H)	12-16	(1.086 Å)	54	$\Delta\theta$(CCO)	13-17-21	(115.0°)
16	Δr(C~C)	13-17	(1.406 Å)	55	$\Delta\theta$(CCO)	14-17-21	(124.9°)
17	Δr(C-O)	13-18	(1.364 Å)	56	$\Delta\theta$(COH)	13-18-20	(107.4°)
18	Δr(C~C)	14-17	(1.389 Å)	57	$\Delta\theta$(COH)	17-21-22	(109.7°)
19	Δr(C-H)	14-19	(1.088 Å)	58	$\Delta\omega$(CNCH)	2-1-5-3	
20	Δr(C-O)	17-21	(1.379 Å)	59	$\Delta\omega$(CCHH)	1-2-6-7	
21	Δr(O-H)	18-20	(0.969 Å)	60	$\Delta\omega$(CCCH)	1-5-9-8	
22	Δr(O-H)	21-22	(0.965 Å)	61	$\Delta\omega$(CCCC)	5-9-11-12	
23	$\Delta\theta$(NCC)	2-1-5	(110.4°)	62	$\Delta\omega$(CCCH)	9-11-14-15	
24	$\Delta\theta$(HCC)	3-1-5	(108.8°)	63	$\Delta\omega$(CCCH)	9-12-13-16	
25	$\Delta\theta$(HCC)	4-1-5	(108.7°)	64	$\Delta\omega$(CCCO)	12-13-17-18	
26	$\Delta\theta$(NCH)	2-1-3	(108.0°)	65	$\Delta\omega$(CCCH)	11-14-17-19	
27	$\Delta\theta$(NCH)	2-1-4	(114.4°)	66	$\Delta\omega$(CCCO)	13-17-14-21	
28	$\Delta\theta$(HCH)	3-1-4	(106.4°)	67	$\Delta\tau$(C-N)	1-2	
29	$\Delta\theta$(CNH)	1-2-6	(109.9°)	68	$\Delta\tau$(C-C)	1-5	
30	$\Delta\theta$(CNH)	1-2-7	(109.6°)	69	$\Delta\tau$(C-C)	5-9	
31	$\Delta\theta$(HNH)	6-2-7	(106.0°)	70	$\Delta\tau$(C~C)	9-11	
32	$\Delta\theta$(CCC)	1-5-9	(112.9°)	71	$\Delta\tau$(C~C)	9-12	
33	$\Delta\theta$(HCC)	8-5-9	(110.7°)	72	$\Delta\tau$(C~C)	11-14	
34	$\Delta\theta$(CCH)	1-5-8	(108.0°)	73	$\Delta\tau$(C~C)	12-13	
35	$\Delta\theta$(CCH)	1-5-10	(108.8°)	74	$\Delta\tau$(C~C)	13-17	
36	$\Delta\theta$(CCH)	9-5-10	(109.6°)	75	$\Delta\tau$(C-O)	13-18	
37	$\Delta\theta$(HCH)	8-5-10	(106.6°)	76	$\Delta\tau$(C~C)	14-17	
38	$\Delta\theta$(CCC)	5-9-11	(121.2°)	77	$\Delta\tau$(C-O)	17-21	
39	$\Delta\theta$(CCC)	5-9-12	(120.2°)				

[a]Δr: stretching, $\Delta\theta$: in-plane deformation, $\Delta\omega$: out-of-plane deformation, $\Delta\tau$: torsion. [b]Molecular structural parameters used for calculation of dopamine *trans* conformer.

Table 3. Local Symmetry Coordinates used for Dopamine (R: the index number of internal coordinates listed in Table 2, S: the index number of local symmetry coordinates adapted, All the redundant local symmetry coordinates are not listed.)

S	Name[a]	Local Sym. Coordinate	Description
1	$\nu(C_{\alpha}\text{-}N)$	R1	C-N stretching
2	$\nu(C_{\alpha}\text{-}C_{\beta})$	R2	C-C stretching
3	$\nu_s(C_{\alpha}H2)$	R3+R4	CH2 sym. Stretching
4	$\nu_a(C_{\alpha}H2)$	R3-R4	CH2 antisym. stretching
5	$\nu_s(NH2)$	R5+R6	NH2 sym. stretching
6	$\nu_a(NH2)$	R5-R6	NH2 antisym. stretching
7	$\nu(C_9\text{-}C_{\beta})$	R7	C-C stretching
8	$\nu_s(C_{\beta}H2)$	R8+R9	CH2 sym. Stretching
9	$\nu_a(C_{\beta}H2)$	R8-R9	CH2 antisym. stretching
10	$\nu(C_9\sim C_{11})$	R10	ring C~C stretching
11	$\nu(C_9\sim C_{12})$	R11	ring C~C stretching
12	$\nu(C_{11}\sim C_{14})$	R12	ring C~C stretching
13	$\nu(C\text{-}H_{15})$	R13	ring C-H stretching
14	$\nu(C_{12}\sim C_{13})$	R14	ring C~C stretching
15	$\nu(C\text{-}H_{16})$	R15	ring C-H stretching
16	$\nu(C_{13}\sim C_{17})$	R16	ring C~C stretching
17	$\nu(C\text{-}O_m)$	R17	C-O stretching
18	$\nu(C_{14}\sim C_{17})$	R18	ring C~C stretching
19	$\nu(C\text{-}H_{19})$	R19	ring C-H stretching
20	$\nu(C\text{-}O_p)$	R20	C-O stretching
21	$\nu(O\text{-}H_m)$	R21	O-H stretching
22	$\nu(O\text{-}H_p)$	R22	O-H stretching
23	$\delta(NCC)$	5R23-R24-R25-R26-R27-R28	N-C-C deformation
24	$\delta_s(C_{\alpha}H2)$	4R28-R24-R25-R26-R27	CH2 scissoring
25	$\delta_w(C_{\alpha}H2)$	R24+R25-R26-R27	CH2 wagging
26	$\delta_r(C_{\alpha}H2)$	-R24+R25-R26+R27	CH2 rocking
27	$\delta_t(C_{\alpha}H2)$	-R24+R25+R26-R27	CH2 twisting
28	$\delta_s(NH2)$	2R31-R29-R30	NH2 sym. bending (scissors)
29	$\delta_a(NH2)$	R29-R30	NH2 antisym.bending (twist)
30	$\delta(CCC)$	5R32-R33-R34-R35-R36-R37	C-C-C deformation
31	$\delta_s(C_{\beta}H2)$	4R37-R33-R34-R35-R36	CH2 scissoring
32	$\delta_w(C_{\beta}H2)$	R33-R34-R35+R36	CH2 wagging
33	$\delta_r(C_{\beta}H2)$	-R33-R34+R35+R36	CH2 rocking
34	$\delta_t(C_{\beta}H2)$	-R33+R34-R35+R36	CH2 twisting
35	$\delta(C_{\beta}\text{-}C\sim C)$	R38	C~C-C bending
36	$\delta(C\sim C_9\sim C)$	R40	ring C~C~C bending
37	$\delta(C\sim C\text{-}H_{15})$	R43	C~C-H bending
38	$\delta(C\sim C\text{-}H_{16})$	R45	C~C-H bending
39	$\delta(C\sim C_{13}\sim C)$	R47	ring C~C~C bending
40	$\delta(C\sim C\text{-}O_m)$	R48	C~C-O bending
41	$\delta(C\sim C_{14}\sim C)$	R50	ring C~C~C bending
42	$\delta(C\sim C\text{-}H_{19})$	R52	C~C-H bending
43	$\delta(C\sim C\text{-}O_p)$	R54	C~C-O bending
44	$\delta(C\text{-}O_m\text{-}H)$	R56	C-O-H bending
45	$\delta(C\text{-}O_p\text{-}H)$	R57	C-O-H bending
46	$\delta(NH2)$	R29+R30+R31	NH2 pseudopuckering (wag)
47	$\gamma(CCCC_5)$	R61	ring-C out-of-plane
48	$\gamma(CCCH_{15})$	R62	ring-H out-of-plane
49	$\gamma(CCCH_{16})$	R63	ring-H out-of-plane
50	$\gamma(CCCO_m)$	R64	ring-O out-of-plane
51	$\gamma(CCCH_{19})$	R65	ring-H out-of-plane
52	$\gamma(CCCO_p)$	R66	ring-O out-of-plane
53	$\tau(\text{-}C_{\alpha}\text{-}N\text{-})$	R67	side chain C-N torsion

Table 3. Continued

S	Name[a]	Local Sym. Coordinate	Description
54	τ(-C_β-C_α-)	R68	side chain C-C torsion
55	τ(-C_9-C_b-)	R69	side chain C-C torsion
56	τ(-C_9~C_{11}-)	R70	ring C~C torsion
57	τ(-C_{12}~C_{13}-)	R73	ring C~C torsion
58	τ(-C_{14}~C_{17}-)	R76	ring C~C torsion
59	τ(-C-O_m-)	R75	hydroxyl C-O torsion
60	τ(-C-O_p-)	R77	hydroxyl C-O torsion

[a] ν: stretching mode, δ: in-plane deformation mode, γ: out-of-plane deformation mode, t: torsion mode, C_α: carbon at α position, C_β: carbon at β position, O_m: oxygen at meta position, O_p: oxygen at para position, ~: carbon-carbon bond in catechol ring. All subscript numbers at the right of atomic symbols are the index numbers indicated in Figure 1.

nates named S1 to S60 was constructed eliminating all the redundant symmetry coordinates. They are 22 stretching modes (symbol name: ν) numbered S1 to S22, 24 in-plane deformation modes (symbol name: δ) numbered S23 to S46, 6 out-of-plane deformation modes (symbol name: γ) numbered S47 to S52, and 8 torsion modes (symbol name: τ) numbered S53 to S60. For the better inspection, we used general chemical symbols C_α and C_β for carbon atoms in the ethylamine moiety and O_p and O_m for oxygen atoms in the catechol moiety, *i.e.*, carbon (1) to C_α, carbon (5) to C_β, oxygen (21) to O_p, and oxygen (18) to O_m. The chemical bond between carbon atoms in the catechol ring was noted to C~C. All subscript numbers at the right of the atomic symbols are the index numbers indicated in Figure 1.

Raw Cartesian force constants matrix obtained from DFT calculation was, as usual, overestimated. The least-square fitting to the experimental frequencies was performed via scaling down the force constants in the internal coordinates converted from a matrix in the Cartesian coordinate. The number of the force constants generated initially in the internal coordinate was 1830 that is the sum of all diagonal and half off-diagonal matrix elements. These are too many to account for, so reduced to a comparable number of force constants using a boundary value in the internal coordinate force constant matrix. The number of force constants out of 1830 could be extracted to 280 for the *trans* conformer, 282 for the *gauche*+ conformer, and 305 for the *gauche*– conformer, respectively, when the absolute value of the off-diagonal matrix elements equal to or greater than 0.05 are survived and all the diagonal matrix elements are included. This boundary value 0.05 was rather arbitrary chosen because the off-diagonal elements less 0.05 are presumed to be minimal enough to be neglected for the structural elucidation. We feel that this gives a comparable and satisfactory set of constraints on the refinement procedure we are trying for a 22-atom system. The number of acting force constants to be considered in the internal coordinate was finally reduced to 305 counting on three different sets of matrix, and then scaled with a proper scale factor. The matrix of these scaled force constants was then transformed to a matrix in the Cartesian coordinate, which was applied to calculate the frequencies using Wilson's *GF* matrix method. This refining procedure was repeated manually until it gave a minimal discrepancy from experimentally observed frequencies. Refined force constants of the diagonal matrix elements and off-diagonal matrix elements in the local symmetry coordinate scheme are shown in Table 4 and Table 5, respectively. Using these values, the frequencies and potential energy distributions were obtained and shown in Table 6 in terms of local symmetry coordinates defined in Table 3. For comparison, scaled frequencies using the exponential scaling method,[23] ω(scaled) = ω_i exp(-$\alpha\omega_i$), where α is the exponent of the exponential scale factor, and ω_i is the calculated frequencies of mode i, were shown in Table 6, together.

Results and Discussion

***Ab initio* Calculations**. The energies of three conformers in the vapor phase, *i.e.*, a stretched *trans*, a folded *gauche*+ and a tightly folded *gauche*– displayed in Figure 2 were calculated from geometries optimized with HF/6-31G**, MP2/6-31G**, and B3LYP/6-31G** functions, respectively, and shown in Table 1. The HF and B3LYP levels with 6-31G** basis functions are affordable for the free energy and the enthalpy change calculations with the frequency test mode, not like MP2 level. So, the free energy and enthalpy values at MP2 level were not calculated. The relative electronic energies (ΔE_{elec} at 298K and 1.0 atm) from HF level are similar for three conformers within 0.2 kcal/mol, favoring the *gauche*+ conformation only 0.12 kcal/mol to the *trans*. But, the *gauche*– conformer is favored in 1.4 kcal/mol to the *trans* when introducing the electron correlation of MP2. The electronic quantities from density functional theory show the *gauche*– conformer is lower in 1.0 kcal/mol for B3LYP level to the *trans*. The *gauche*+ and *gauche*– conformer have the very close values less 0.02 kcal/mol in the electronic quantities.

Counting the enthalpy change (ΔH_T) corrected with thermal quantity (+RT) and the entropy effect (-$T\Delta S$), the free energies (ΔG_T at 298K and 1.0 atm) are closely similar and the differences are minimal to about 0.3 kcal/mol. The *trans* conformation is favored in 0.24 kcal/mol to the *gauche*+ and *gauche*– at HF level, but the *gauche*+ conformation is lower in 0.33 kcal/mol to the *trans* at B3LYP level. The free energies for the *gauche*+ and *gauche*– conformations are as well very close to each other within 0.02 kcal/mol at both HF and

Table 4. Refined Diagonal Force Constants (mdyne/Å or Equivalent unit for bending or torsion) (S: the index number of local symmetry coordinates listed in Table 3)

(S, S)	Force	(S, S)	Force	(S, S)	Force
(1, 1)	4.7286	(2, 2)	3.5143	(3, 3)	4.8150
(4, 4)	4.7280	(5, 5)	5.2900	(6, 6)	5.1730
(7, 7)	4.1980	(8, 8)	4.6600	(9, 9)	4.6610
(10,10)	6.7170	(11,11)	6.4135	(12,12)	6.5914
(13,13)	5.0170	(14,14)	6.9006	(15,15)	5.0860
(16,16)	6.5130	(17,17)	6.1006	(18,18)	7.0480
(19,19)	4.9650	(20,20)	5.6848	(21,21)	6.2551
(22,22)	6.2610	(23,23)	0.9889	(24,24)	0.5911
(25,25)	0.6781	(26,26)	0.9656	(27,27)	0.6759
(28,28)	0.6308	(29,29)	0.7858	(30,30)	0.9908
(31,31)	0.5867	(32,32)	0.5115	(33,33)	0.6636
(34,34)	0.5078	(35,35)	1.5316	(36,36)	3.1360
(37,37)	1.0815	(38,38)	1.0063	(39,39)	3.5200
(40,40)	1.9589	(41,41)	3.0931	(42,42)	1.0761
(43,43)	2.1196	(44,44)	0.8817	(45,45)	0.7676
(46,46)	0.7089	(47,47)	3.8503	(48,48)	3.3725
(49,49)	3.2509	(50,50)	3.9083	(51,51)	3.3223
(52,52)	3.8272	(53,53)	0.0745	(54,54)	0.3359
(55,55)	0.1562	(56,56)	0.8022	(57,57)	0.7318
(58,58)	0.8053	(59,59)	0.1594	(60,60)	0.0138

Table 5. Refined Off-Diagonal Force Constants (mdyne/Å or Equivalent unit for bending or torsion) (S: the index number of local symmetry coordinate listed in Table 3)

(S, S)	Force	(S, S)	Force	(S, S)	Force
(2, 1)	0.2729	(3, 1)	0.2119	(3, 2)	0.1250
(5, 1)	0.0490	(7, 2)	0.3055	(8, 2)	0.1102
(8, 7)	0.0814	(10, 7)	0.1803	(11, 7)	0.1744
(11,10)	1.0336	(12,10)	0.6453	(12,11)	-0.4320
(13,10)	0.1292	(13,12)	0.1240	(14,10)	-0.5378
(14,11)	0.5906	(14,13)	-0.0546	(15,11)	0.1345
(15,12)	-0.0569	(15,14)	0.1195	(16,11)	-0.5402
(16,12)	-0.4716	(16,13)	-0.0462	(16,14)	0.8785
(17,12)	0.1122	(17,14)	0.3925	(17,16)	0.2976
(18,10)	-0.6623	(18,11)	-0.0442	(18,12)	0.9501
(18,14)	-0.5357	(18,15)	-0.0636	(18,16)	0.6185
(19,12)	0.0661	(19,18)	0.0601	(20,10)	-0.2287
(20,11)	-0.1300	(20,16)	0.5872	(20,17)	0.0996
(20,18)	0.4731	(21,17)	0.0884	(22,16)	-0.0560
(23, 1)	0.2696	(23, 2)	0.2264	(23, 3)	-0.0900
(23, 5)	-0.0601	(23, 9)	-0.0687	(24, 1)	-0.2213
(24, 2)	-0.1388	(24, 3)	0.0995	(25, 1)	-0.4302
(25, 2)	0.1907	(26, 4)	-0.1586	(26, 6)	-0.0656
(27,26)	0.0664	(28, 1)	-0.2485	(28, 5)	0.1355
(29, 6)	0.0971	(29,26)	-0.1216	(29,27)	-0.0284
(30, 2)	0.2642	(30, 4)	-0.0563	(30, 7)	0.0189
(30, 8)	-0.0977	(30,23)	0.0385	(30,27)	0.0487
(31, 2)	-0.0973	(31, 7)	-0.0954	(31, 8)	0.1026
(32, 2)	-0.1959	(32, 7)	0.2842	(33, 1)	0.0010
(33, 2)	0.0267	(33, 9)	-0.1489	(33,26)	0.0969
(33,30)	0.0619	(34,23)	-0.2929	(35, 2)	-0.0740
(35, 9)	0.0963	(35,10)	0.3174	(35,11)	-0.2956
(35,16)	0.0370	(35,21)	-0.0454	(35,30)	-0.0360

Table 5. Continued

(S, S)	Force	(S, S)	Force	(S, S)	Force
(35,34)	-0.0492	(36, 7)	-0.3620	(36,10)	0.9681
(36,11)	0.5179	(36,12)	-0.3283	(36,13)	0.1287
(36,14)	-0.3081	(36,15)	0.1850	(36,16)	-0.4653
(36,18)	-0.4846	(36,20)	-0.1947	(36,30)	0.0360
(36,32)	-0.0356	(36,34)	-0.1342	(36,35)	0.7826
(37,10)	-0.5307	(37,11)	-0.0480	(37,14)	0.1756
(37,16)	0.2017	(37,18)	0.0540	(37,36)	-0.4441
(38,10)	0.1261	(38,12)	0.2226	(38,14)	-0.4091
(38,16)	-0.0012	(38,18)	0.1985	(38,36)	-0.2420
(39,10)	-0.5727	(39,11)	-0.4313	(39,12)	-0.4679
(39,14)	0.8998	(39,15)	0.1364	(39,16)	0.3543
(39,17)	-0.5354	(39,20)	0.2911	(39,21)	0.0599
(39,36)	-0.1350	(39,37)	0.1264	(39,38)	-0.3046
(40,11)	-0.1790	(40,14)	0.2657	(40,16)	-0.4444
(40,17)	0.0448	(40,18)	0.1306	(40,21)	0.0583
(40,35)	0.0565	(40,36)	-0.2823	(40,38)	-0.0005
(40,39)	1.0570	(41,10)	-0.3354	(41,11)	-0.4337
(41,12)	0.5149	(41,13)	0.1343	(41,14)	-0.4992
(41,16)	-0.2133	(41,18)	1.0321	(41,19)	-0.1834
(41,20)	0.3258	(41,22)	-0.0716	(41,35)	-0.1721
(41,36)	0.0031	(41,37)	-0.2569	(41,38)	0.1821
(41,39)	0.1319	(41,40)	0.1426	(42,11)	0.0492
(42,12)	-0.2262	(42,18)	0.1917	(42,36)	0.1078
(42,39)	-0.0562	(42,41)	0.4546	(43,10)	0.2655
(43,11)	0.4350	(43,16)	0.1516	(43,17)	-0.2247
(43,18)	-0.7369	(43,20)	0.2534	(43,22)	0.1087
(43,36)	0.2760	(43,39)	-0.5049	(43,41)	-0.5951
(44,17)	0.4529	(44,21)	0.2260	(44,40)	0.0272
(44,43)	-0.0457	(45,20)	0.3540	(45,22)	0.1436
(45,43)	-0.0068	(46, 1)	0.4924	(46, 5)	0.3467
(47, 2)	-0.0547	(47, 7)	0.0255	(47,11)	-0.1496
(47,14)	-0.0556	(47,16)	0.0832	(47,17)	0.0414
(47,21)	-0.1116	(47,23)	-0.0260	(47,26)	-0.0163
(47,30)	0.0123	(47,32)	-0.0289	(47,35)	0.0810
(47,36)	0.1145	(47,39)	-0.1607	(47,40)	-0.1547
(47,43)	0.1113	(47,44)	0.0798	(48,30)	-0.1340
(48,39)	0.0514	(48,40)	0.0979	(48,47)	-0.1788
(49, 1)	-0.0320	(49,23)	-0.0834	(49,35)	-0.0786
(49,40)	-0.0954	(49,47)	0.4233	(49,48)	0.4779
(50,47)	-0.4816	(50,48)	0.5827	(50,49)	0.4644
(51,47)	0.3230	(51,48)	0.7697	(51,49)	0.6274
(51,50)	0.6621	(52,47)	-0.5176	(52,48)	0.2530
(52,49)	-0.6493	(52,50)	0.4737	(52,51)	-0.5799
(54,33)	0.1530	(54,47)	-0.0102	(55,23)	0.0053
(55,30)	-0.0221	(56,30)	-0.1536	(56,47)	0.4386
(56,48)	0.4580	(56,49)	0.4546	(56,50)	0.1490
(56,51)	0.2966	(56,52)	-0.1275	(57,30)	0.0402
(57,35)	-0.0019	(57,47)	-0.1878	(57,48)	0.0168
(57,49)	-0.2671	(57,50)	0.0828	(57,51)	-0.1567
(57,52)	0.4924	(58,47)	0.0725	(58,48)	-0.3320
(58,49)	-0.1684	(58,50)	-0.5077	(58,51)	-0.5501
(58,52)	-0.0808	(59,35)	-0.1043	(59,47)	-0.0965
(59,48)	0.0828	(59,50)	0.0408	(59,52)	-0.0360
(60,49)	0.0822	(60,52)	0.0025		

Table 6. Observed Raman and Calculated Frequencies (cm^{-1}) of Dopamine and Potential Energy Distribution (%)

Obs.	Calc.[a]	Calc.[b]	Potential Energy Distribution (greater than 5.0%)[c]
3345	3502	3346	100 ν(O-Hp)
3343	3450	3343	100 ν(O-Hm)
3081	3270	3081	100 ν_a(NH2)
3054	3198	3054	100 ν_s(NH2)
3044	2960	3044	99 ν(C-H_{16})
3025	2953	3025	92 ν(C-H_{15}), 7 n(C-H_{19})
3008	2931	3008	93 ν(C-H_{19}), 7 n(C-H_{15})
2963	2861	2964	100 ν_a(C_βH2)
2938	2849	2938	98 ν_a(C_αH2)
2923	2821	2922	98 ν_s(C_βH2)
2876	2813	2876	100 ν_s(C_αH2)
1617	1610	1617	28 ν(C_{12}~C_{13}), 19 ν(C_{11}~C_{14}), 12 δ(C~C-H_{19}), 11 n(C_{13}~C_{17}), 8 δ(C-O_m-H), 7 δ(C~C_9~C), 7 ν(C_{14}~C_{17}), 6 ν(C_9~C_{11}), 5 δ(C~C-H_{16})
1602	1608	1602	97 δ_s(NH2)
1581	1591	1581	26 ν(C_{14}~C_{17}), 24 ν(C_{13}~C_{17}), 15 δ(C~C_{13}~C), 14 ν(C_9~C_{11}), 14 ν(C_9~C_{12}), 8 δ(C~C-O_p), 7 ν(C-O_m), 7 δ(C~C_{14}~C), 7 δ(C~C-H_{15})
1496	1504	1496	20 δ(C~C-H_{19}), 16 δ(C~C-H_{15}), 15 δ(C~C-H_{16}), 12 ν(C_{14}~C_{17}), 10 ν(C-O_p), 10 ν(C_9~C_{11}), 8 ν(C_9~C_{12}), 7 d(C~C_9~C), 7 ν(C_{13}~C_{17}), 5 ν(C_{12}~C_{13}), 5 n(C_9-C_b)
1470	1456	1471	90 δ_s(C_βH2)
1457	1446	1457	34 δ_s(C_αH2), 13 δ(C-O_m-H), 11 ν(C_{11}~C_{14}), 11 (C_{12}~C_{13}), 6 δ(C~C-H_{19}), 5 δ(C~C-H_{15})
1449	1442	1450	57 δ_s(C_αH2), 10 δ(C-O_m-H), 8 ν(C_{11}~C_{14}), 7 ν(C_{12}~C_{13})
1350	1357	1350	20 δ_a(NH2), 12 δ_t(C_αH2), 9 δ_r(C_aH2), 8 δ(C~C-H_{15}), 7 ν(C_9~C_{11}), 6 ν(C_9-C_b), 6 δ_w(C_αH2)
1341	1353	1341	93 δ_w(C_αH2)
*	1343	1332	27 δ(C-O_p-H), 22 δ(C~C-H_{16}), 16 δ(C~C-H_{15}), 15 ν(C_{14}~C_{17}), 9 ν(C_9~C_{12}), 6 δ(C~C-H_{19}), 6 δ(C~C-O_p), 6 ν(C_9~C_{11}), 5 ν(C_{13}~C_{17})
1322	1315	1322	21 ν(C_9~C_{11}), 19 δ_a(NH2), 13 δ(C-O_m-H), 12 ν(C_9~C_{12}), 7 δ(C~C-H_{16}), 6 δ_t(C_βH2), 5 δ_r(C_αH2)
1287	1308	1288	42 ν(C-O_m), 11 ν(C_9~C_{12}), 11 δ(C~C_{13}~C), 11 δ(C-O_m-H), 9 δ(C~C-H_{19}), 8 ν(C_{13}~C_{17}), 6 ν(C_{11}~C_{14}), 6 ν(C_9-C_b), 6 δ(C~C-H_{15})
1272	1284	1272	30 ν(C-O_p), 20 δ(C~C-H_{19}), 12 δ(C-O_m-H), 8 δ(C~C_{13}~C), 7 ν(C_{11}~C_{14}), 6 δ(C-O_p-H)
1260	1254	1260	70 δ_t(C_αH2), 21 δ_a(NH2)
1206	1206	1205	20 δ_t(C_βH2), 17 δ(C-O_p-H), 8 ν(C_{12}~C_{13}), 8 δ(C-O_m-H), 7 ν(C_9-C_b), 6 ν(C_α-N), 6 ν(C_{13}~C_{17}), 5 δ_w(C_βH2)
1187	1182	1187	22 ν(C_{12}~C_{13}), 20 δ(C-O_m-H), 18 δ(C~C-H_{16}), 6 ν(C_{13}~C_{17}), 6 δ_w(C_βH2), 6 ν(C_9~C_{11}), 5 ν(C-O_p), 5 ν(C_9~C_{12})
1175	1152	1175	22 ν(C_{11}~C_{14}), 19 δ(C-O_p-H), 15 δ(C~C-H_{15}), 13 δ(C~C-H_{19}), 8 ν(C-O_p), 7 ν(C_{14}~C_{17}), 6 ν(C_9~C_{11}), 6 δ_w(C_βH2)
1152	1141	1152	74 δ_w(C_βH2), 8 ν(C_α-C_β), 6 ν(C_{11}~C_{14})
1147	1123	1146	25 ν(C_9-C_b), 10 δ(C~C-H_{16}), 9 ν(C_{11}~C_{14}), 9 ν(C_α-N), 8 δ_t(C_βH2), 8 ν(C_9~C_{11})
1115	1103	1115	21 δ(C~C_{14}~C), 17 δ(C-O_p-H), 12 ν(C_9~C_{12}), 11 δ(C~C-H_{15}), 9 δ(C~C_{13}~C), 9 ν(C-O_p), 9 ν(C_{14}~C_{17}), 6 δ(C~C-O_m)
1014	1065	1014	43 ν(C_α-N), 23 δ_t(C_βH2), 21 ν(C_α-C_β)
961	993	960	27 δ_t(C_αH2), 15 δ_a(NH2), 9 ν(C_9~C_{11}), 6 ν(C-O_m), 5 δ(CCC), 5 τ(-C_β-C_α-)
948	946	948	22 δ(NH2), 14 δ_t(C_βH2), 9 ν(C-O_m), 9 ν(C_9-C_β), 9 ν(C_α-C_β), 7 δ(C~C_9~C), 7 δ_r(C_αH2)
932	899	932	49 δ(NH2), 13 δ_r(C_αH2), 10 ν(C_α-C_β), 9 ν(C_α-N), 6 δ_a(NH2), 5 δ_r(C_βH2)
876	891	877	67 γ(CCCH_{16}), 28 τ(-C_{12}~C_{13}-), 14 γ(CCCH_{15})
853	865	853	59 γ(CCCH_{15}), 29 γ(CCCH_{19}), 25 τ(-C_9~C_{11}-), 13 γ(CCCH_{16}), 9 τ(-C_{14}~C_{17}-), 6 τ(-C_{12}~C_{13}-)
813	842	813	35 ν(C_α-C_β), 33 ν(C_α-N), 20 δ(NH2)
796	835	796	64 γ(CCCH_{19}), 36 τ(-C_{14}~C_{17}-), 13 τ(-C_9~C_{11}-), 12 γ(CCCH_{15})
772	786	773	35 δ_r(C_βH2), 11 δ(C~C_9~C), 8 ν(C-O_p), 7 δ_r(C_αH2), 6 ν(C_α-N), 6 γ(CCCH_{19})
751	780	750	23 ν(C_{13}~C_{17}), 18 δ_r(C_βH2), 13 δ(C~C_{14}~C), 9 ν(C-O_p), 9 δ(C~C_9~C), 7 ν(C_{14}~C_{17}), 6 ν(C-O_m)
724	706	724	16 δ(C~C_{14}~C), 13 δ_r(C_αH2), 12 ν(C_9-C_β), 10 δ(CCC), 9 δ_r(C_βH2), 8 γ($CCCC_5$), 6 ν(C_9~C_{11})
*	691	668	31 γ($CCCC_5$), 12 δ(C~C_{14}~C), 10 γ(CCCO_m), 9 γ(CCCO_p), 9 τ(-C_{12}~C_{13}-), 7 δ(CCC), 5 γ(CCCH_{15})
633	631	633	50 γ(CCCO_m), 42 γ(CCCO_p), 8 τ(-C-O_m-), 7 $_t$(-C_{14}~C_{17}-)
597	585	597	45 τ(-C-O_m-), 11 δ(C~C_{13}~C), 10 δ(C~C-O_p)
570	520	571	39 τ(-C-O_m-), 23 δ(C~C_{13}~C), 14 δ(C~C-O_p), 6 δ(C~C_{14}~C), 6 ν(C_{14}~C_{17})
550	471	550	13 δ(C~C_{14}~C), 10 δ(C~C-O_m), 10 τ(-C_9~C_{11}-), 7 δ(CCC), 7 δ(C~C_9~C), 6 δ(C~C-O_p), 6 γ($CCCC_5$), 5 γ(CCCH_{15}), 5 δ(C_β-C~C)
475	455	475	22 δ(C~C_{13}~C), 22 δ(C~C-O_m), 7 δ(C_β-C~C), 7 δ(NCC), 7 τ(-C-O_m-), 6 γ(CCCH_{15}), 6 τ(-C_{14}~C_{17}-), 5 δ_r(C_βH2)
460	434	460	23 γ(CCCO_p), 17 γ(CCCO_m), 9 δ(NCC), 7 τ(-C_{12}~C_{13}-), 5 δ(C~C_{13}~C)

Table 6. Continued

Obs.	Calc.[a]	Calc.[b]	Potential Energy Distribution (greater than 5.0%)[c]
396	423	398	34 δ(C~C_9~C), 14 γ(CCCO_p), 7 δ(C~C_{13}~C), 7 ν(C_9-C_β), 7 τ(-C_9~C_{11}-), 7 τ(-C_{14}~C_{17}-), 6 γ(CCCO_m)
390	365	391	41 δ(NCC), 13 δ_t(C_βH2), 11 δ(C~C_9~C), 11 τ(-C_β-C_α-), 10 δ(C~C_{13}~C), 9 δ(C~C-O_m), 8 τ(-C_9-C_β-), 7 δ(C_β-C~C)
333	338	334	19 τ(-C_β-C_α-), 15 τ(-C_α-N-), 11 δ(NCC), 10 τ(-C_{14}~C_{17}-), 7 γ(CCCO_p), 6 τ(-C_{12}~C_{13}-)
312	307	308	47 δ(C~C-O_p), 38 δ(C~C-O_m)
267	290	267	65 τ(-C_α-N-), 18 δ(C_β-C~C), 8 δ(C~C-O_m)
*	252	225	29 τ(-C_{12}~C_{13}-), 19 δ(NCC), 15 δ(C_β-C~C), 14 δ(CCC), 11 γ(CCCH_{16}), 5 γ(CCCO_p)
204	202	203	17 δ(C_β-C~C), 14 τ(-C_{14}~C_{17}-), 13 τ(-C_{12}~C_{13}-), 9 γ(CCCC_5), 6 δ(CCC), 6 τ(-C-O_p-)
157	182	157	51 τ(-C-O_p-), 19 τ(-C_β-C_α-), 16 γ(CCCH_{16}), 13 δ(C_β-C~C), 8 τ(-C_9~C_{11}-)
*	128	146	57 τ(-C-O_p-), 15 τ(-C_β-C_α-), 8 γ(CCCH_{16}), 8 τ(-C_{14}~C_{17}-), 6 δ(C_β-C~C)
*	81	74	37 τ(-C_9~C_{11}-), 34 γ(CCCC_5), 27 δ(CCC), 9 τ(-C_β-C_α-), 6 γ(CCCH_{16})
*	46	61	76 τ(-C_9-C_β-), 9 δ_r(C_βH2), 5 τ(-C_β-C_α-)

[a]Calculated frequencies using the exponential scaling method upon Reference 23. [b]Calculated frequencies in this work. [c]Symbols are corresponding to the names listed in Table 3. *Not observed bands.

B3LYP level. The dipole moment shows the highest values for stretched *trans* conformation, less for the folded *gauche*+, and the smallest values for the tightly folded *gauche*– from all three different methods as predicted from the structural considerations.

These calculated results could imply that three conformers in neutral species have almost the same energy, and that the populations are evenly distributed for each of three conformers. The actual structure that can be seen in powder states is dependent strongly on the counter ions, Cl^- ions or the molecule HCl mixed with sample. The polar HCl molecules or Cl^- ions with moderate charge density nearby could interact with dopamine neutral base molecule to form a stable conformer, possibly the *trans* conformer because it has the largest dipole moment among three.

Spectral Analysis and Normal Mode Analysis. Because dopamine does not have any symmetry, all the vibrational bands are Raman and infrared active. The structure of dopamine is labile to the rotation through the C_α-C_β bond, so it can have one of three different staggered conformations as shown in Figure 2. A close inspection of calculated spectra of (A) *gauche*–, (B) *gauche*+, and (C) *trans* conformer in Figure 3 reveals a clear distinction in the region of 2800-3000 cm^{-1}, the stretching region of two methylene groups in the ethylamine moiety, *i.e.*, -$C_\alpha H_2$- and -$C_\beta H_2$-. They can be designated to four stretching modes, symmetric and anti-symmetric for each methylene. However, three carbon-hydrogen stretching modes of the catechol ring, the symmetric and anti-symmetric stretching of -NH_2 terminal group, and two oxygen-hydrogen stretching modes of the catechol moiety are almost the same in the frequency and the band intensity for three conformers. The rotation through the C_α-C_β bond seems to develop quite different force field environments on the methylene stretching modes in the case of the *trans* from other conformers. This fact may be convincing when one regards the structural aspects of three conformers shown in Figure 2.

We could observe that the stretching frequencies except stretching modes of two methylene groups are far apart from the experimental ones shown in Raman spectrum (B) of Figure 4. In fact, it needs further scaling even though they were displayed with scaled 0.96 times to frequencies calculated using the raw force constant matrix. We follow the assignments of normal mode analysis for this region because the stretching modes are strongly correlated with the characteristic group frequencies and their potential energy distributions are highly localized over 90% to corresponding stretching modes as shown in Table 6. The O-H stretching frequencies come out closely located at 3345.1 for O-H_p and 3343.1 cm^{-1} for O-H_m, respectively. Their diagonal force constants are minimally different, 6.261 and 6.255 mdyne/Å for each. But, the C-O_m bond is a little stronger than C-O_p bond as can be seen in the force constants 6.1006 and 5.6848 mdyne/Å. It has been known that the proton at O-H_m is more acidic than at O-H_p in the hydrated state of dopamine. This reveals that the acidity of a hydroxyl proton is due to the C-O bond characters. The force constants of carbon-carbon bonds in a catechol ring show that the *p*-electrons responsible for the double bond character are considerably localized on the C_{14}~C_{17}, C_{12}~C_{13}, and C_9~C_{11} bonds. This result shows the catechol ring is well distorted from the symmetric benzene ring structure. The diagonal force constants for two CH_2 symmetric stretching modes at α and β carbons are obtained to be 4.8150 and 4.6600, respectively. This is in good agreement to the the case of ethylmethyl amine,[20] where as 4.5634.

In 1600 cm^{-1} region, three are three bands that are Raman and infrared active in intensity. A band at 1601.7 cm^{-1} is attributed to highly localized symmetric deformation (scissoring) of terminal NH_2 which is strongly correlated to C-N stretching and NH_2 symmetric stretching modes. The symmetric deformation of NH_2 usually occurs in the region 1590 -1650 cm^{-1} strong in infrared, but weak in Raman for the primary aliphatic amines. Both Raman and infrared spectra obtained in this experiment as well in the calculated show moderate intensities for this scissoring mode, however. Other two at 1617.1 and 1580.5 cm^{-1} are assigned to the ring stretching modes, mostly attributed to the ring carbon-carbon stretching modes about 80%.

Other deformations of amine NH_2 are an anti-symmetric

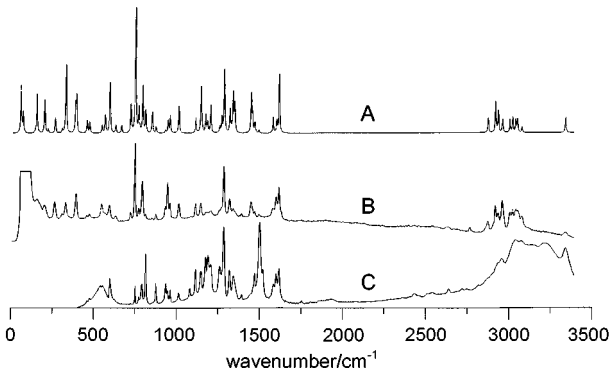

Figure 4. (A) Constructed Raman spectrum of dopamine neutral base using force constant matrix from the refinement procedure and intensities from DFT frequency calculation; (B) Experimental Fourier transform Raman spectrum in powder state obtained at 4 cm^{-1} resolution using cw 1064 nm Nd:YAG laser excitation; (C) Experimental Fourier transform infrared spectrum in KBr pellet obtained in an absorbance scale at 4 cm^{-1} resolution.

deformation (twisting) and a pseudo-puckering (wagging) mode. This wagging mode is mostly localized into two bands at 932 and 948 cm^{-1}, and strongly correlated to C-N stretching and NH_2 symmetric stretching modes. The twisting mode is widely distributed to bands at 1350.0, 1322.0, 1260.0, and 961.0 cm^{-1}, weakly correlated to NH_2 anti-symmetric stretching, $C_\alpha H_2$ rocking, and $C_\alpha H_2$ twisting modes.

The stretching modes of two C-C bonds in the ethylamine side-chain are correlated to each other as well to C-N stretching mode, very widely distributed to at 1495.6, 1350.0, 1287.0, 1206.0, 1152.0, 1013.5, 948.0, 932.0, 813.0, and 724 cm^{-1}. The deformations of a CH_2 group in the ethylamine side-chain are scissoring, wagging, twisting and rocking modes. The scissoring and wagging modes of a CH_2 group at β-carbon are localized to bands at 1470.0 and 1152.0 cm^{-1}, respectively. However, the twisting mode is widely distributed to many bands in the range of 1322.0 to 948.0 cm^{-1}, and the rocking mode is in the range of 932 to 475 cm^{-1}. The scissoring, wagging, and twisting modes at a-carbon are localized to bands at 1449.0, 1341.0 and 1260.0 cm^{-1}, respectively. The rocking mode is distributed in the range of 1350.0 to 724.0 cm^{-1}. The scissoring deformations[21] of two CH_2 groups in the histamine monohydrochloride cation as a microcrystalline powder were assigned to 1455 and 1441 cm^{-1}, respectively. In this case of neutral base form of dopamine, they are observed and assigned to two bands at 1470 and 1449 cm^{-1} in localized modes. The wagging and twisting modes are observed and reported in the range of 1100-1400 cm^{-1}, and the rocking modes are in 1100-700 cm^{-1} for the extended polymethylene chain.[22]

In-plane deformations (noted in δ) of a catechol ring and an ethylamine moiety, out-of-plane deformations (noted in γ) of six elements attached to the ring carbons, and torsion motions (noted in τ) of a side chain and a catechol ring are well distributed and mixed to generate all the bands in the mid and low frequency regions. The skeletal deformations (δ(NCC) and δ(CCC)) and skeletal torsions (τ(-C_α-N-), τ(-C_β-C_α-), and τ(-C_9-C_β-)) of a side chain are distributed in the range of less than 500 cm^{-1}.

Conclusions

Ab initio calculations performed with 6-31G** basis set at HF, MP2, and B3LYP show minimal relative stability for a stretched *trans*, a folded *gauche*+, and a folded *gauche*– conformer of dopamine neutral base in isolated state. The density functional force field with the experimental Raman and infrared spectra enables one to obtain a detailed force field to clarify the structure of dopamine in powder state. The *trans* conformation is preferred in this case. All the bands are assigned from a refining procedure of the force constant matrix.

References

1. Grol, C. J. *The Chemistry of Dopamine*; Horn, A. S., Korf, J., Westerink, B. H. C., Eds.; Academic press: New York, U. S. A., 1979; p 7.
2. (a) Rajan, K. S.; Davis, J. M.; Colburn, R. W. *J. Neurochem.* **1974**, *22*, 137. (b) Rajan, K. S.; Skripkus, A.; Marks, G. E.; Davis, J. M. *Bioinorg. Chem.* **1976**, *6*, 93. (c) Park, M. K.; Yoo, H. S.; Kang, Y. K.; Lee, N. S. *Bull. Korean Chem. Soc.* **1992**, *13*, 230.
3. Youn, M. Y.; Kim, Y.; Lee, N. S. *Bull. Korean Chem. Soc.* **1997**, *18*, 1314.
4. Lee, N. S.; Hsieh, Y. Z.; Paisley, R. F.; Morris, M. D. *Anal. Chem.* **1988**, *60*, 442.
5. Que, L.; Heistand, R. H. *J. Am. Chem. Soc.* **1979**, *101*, 2219.
6. Urban, J. J.; Cramer, C. J.; Famini, G. R. *J. Am. Chem. Soc.* **1992**, *114*, 8226.
7. Nishihira, J.; Tachikawa, H. *J. Theor. Biol.* **1997**, *185*, 157.
8. Cramer, C. J.; Truhlar, D. G. *J. Am. Chem. Soc.* **1991**, *113*, 8305.
9. Alagone, G.; Ghio, C. *J. Chem. Phys.* **1996**, *204*, 239.
10. Fausto, R.; Ribeiro, M. S.; Pedroso de Lima, J. J. *J. Mol. Struct.* **1999**, *484*, 181.
11. Urban, J. J.; Cronin, C. W.; Roberts, R. R.; Famini, G. R. *J. Am. Chem. Soc.* **1997**, *119*, 12292.
12. Nagy, P. I.; Alagona, G.; Ghio, C. *J. Am. Chem. Soc.* **1999**, *121*, 4804.
13. Collado, J. A.; Tunon, L.; Silla, E.; Ramirez, F. J. *J. Phys. Chem. A* **2000**, *104*, 2120.
14. Ceccarelli, M.; Lutz, M.; Marchi, M. *J. Am. Chem. Soc.* **2000**, *122*, 3532.
15. Zanoun, A.; Lagant, P.; Vergoten, G. *J. Mol. Struct.* **1999**, *510*, 85.
16. Han, W. G.; Jalkanen, K. J.; Elstner, M.; Suhai, S. *J. Phys. Chem. B* **1998**, *102*, 2587.
17. Durig, J. R.; Yu, Z.; Guirgis, G. A. *J. Phys. Chem. A* **2000**, *104*, 741.
18. Lee, S.-H.; Krimm, S. *Biopolymer* **1998**, *48*, 283.
19. Wilson, Jr., E. R.; Decius, J. C.; Cross, P.C. *Molecular Vibrations*; Dover Publications Inc.: New York, U. S. A., 1955.
20. Batista de Carvalho, L. A. E.; Teiseira-Dias, J. J. C. *J. Raman Spectrosc.* **1995**, *26*, 653.

21. Collado, J. A.; Ramirez, F. J. *J. Raman Spectrosc*. **1999**, *30*, 391.
22. Shimanouchi, T. *Pure Appl. Chem*. **1963**, *7*, 131.
23. (a) Lee, J. Y.; Hahn, O.; Lee, S. J.; Choi, H. S.; Shim, H.; Mhin, B. J.; Kim, K. S. *J. Phys. Chem*. **1995**, *99*, 1913. (b) Lee, J. Y.; Hahn, O.; Lee, S. J.; Mhin, B. J.; Lee, M. S.; Kim, K. S. *ibid* **1995**, *99*, 2262.